

AD-A220 270

Development of an All Silicon Integrated
Optical Modulator
for High Speed Data Communications
and Sensor Applications

Final Report

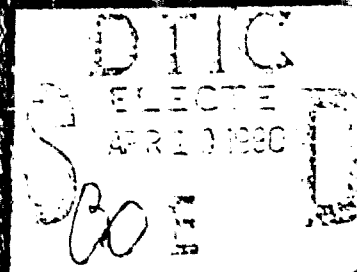
BEST
AVAILABLE COPY

Edward L. Ginzton Laboratory

OF THE

W.W. HANSEN LABORATORIES OF PHYSICS

STANFORD UNIVERSITY, STANFORD, CALIFORNIA 94305



DISTRIBUTION STATEMENT A

Approved for public release
Distribution Unlimited

2

**Development of an All Silicon Integrated
Optical Modulator
for High Speed Data Communications
and Sensor Applications**

Final Report

**O. Solgaard, J. I. Thackara, A. A. Godil,
B. R. Hemenway, and D. M. Bloom**

January, 1990

U. S. Army Research Office

Under Contract #DAAL03-88-K-0120

Leland Stanford Jr. University

**Approved for Public Release;
Distribution Unlimited**



The view, opinions, and/or findings contained in this report are those of the author(s) and should not be construed as an official Department of the Army position, policy, or decision, unless so designated by other documentation.

UNCLASSIFIED

MASTER COPY

FOR REPRODUCTION PURPOSES

SECURITY CLASSIFICATION OF THIS PAGE

REPORT DOCUMENTATION PAGE

1a. REPORT SECURITY CLASSIFICATION Unclassified		1b. RESTRICTIVE MARKINGS	
2a. SECURITY CLASSIFICATION AUTHORITY		3. DISTRIBUTION / AVAILABILITY OF REPORT Approved for public release; distribution unlimited.	
2b. DECLASSIFICATION / DOWNGRADING SCHEDULE		4. PERFORMING ORGANIZATION REPORT NUMBER(S)	
4. PERFORMING ORGANIZATION REPORT NUMBER(S)		5. MONITORING ORGANIZATION REPORT NUMBER(S) ARO 26088.4-PH	
6a. NAME OF PERFORMING ORGANIZATION Leland Stanford University	6b. OFFICE SYMBOL (If applicable)	7a. NAME OF MONITORING ORGANIZATION U. S. Army Research Office	
6c. ADDRESS (City, State, and ZIP Code) Stanford University Stanford, CA 94305-4085		7b. ADDRESS (City, State, and ZIP Code) P. O. Box 12211 Research Triangle Park, NC 27709-2211	
8a. NAME OF FUNDING/SPONSORING ORGANIZATION U. S. Army Research Office	8b. OFFICE SYMBOL (If applicable)	9. PROCUREMENT INSTRUMENT IDENTIFICATION NUMBER DAAL03-88-K-0120	
8c. ADDRESS (City, State, and ZIP Code) P. O. Box 12211 Research Triangle Park, NC 27709-2211		10. SOURCE OF FUNDING NUMBERS	
		PROGRAM ELEMENT NO.	PROJECT NO.
		TASK NO.	WORK UNIT ACCESSION NO.
11. TITLE (Include Security Classification) Development of an All Silicon Integrated Optical Modulator for High Speed Data Communications and Sensor Applications. Unclassified			
12. PERSONAL AUTHOR(S) B. R. Hemenway, O. Solgaard, A. A. Godil, J. I. Thackara, and D. M. Bloom			
13a. TYPE OF REPORT Final	13b. TIME COVERED FROM 8/88 TO 11/90	14. DATE OF REPORT (Year, Month, Day) 90-1-31	15. PAGE COUNT 41
16. SUPPLEMENTARY NOTATION The view, opinions and/or findings contained in this report are those of the author(s) and should not be construed as an official Department of the Army position, policy, or decision, unless so designated by other documentation.			
17. COSATI CODES		18. SUBJECT TERMS (Continue on reverse if necessary and identify by block number)	
FIELD	GROUP	SUB-GROUP	
19. ABSTRACT (Continue on reverse if necessary and identify by block number) During the one year and three months that the project on the "Development of an All Silicon Integrated Optical Modulator for High Speed Data Communications and Sensor Applications" has been running, the goals for the project have all been met. The first generation silicon light intensity modulator had a modulation depth of up to 30% in a bandwidth up to 200 MHz. In accordance with the intents of the project, the modulator occupied a small surface area and is fabricated using standard silicon technology, making the modulator suitable for integration with silicon integrated circuits. The second generation of the modulator had several refinements, among which the push-pull design proved to be the most worth while, giving a doubling of the modulation depth. In the design of the modulator special emphasis was put on easy interfacing with fiber optics, and it was demonstrated that the modulator could not only simply and inexpensively be directly coupled to single mode optical fibers (pigtailling), but that the direct coupling of the modulators was more effective and led to a higher modulation index (24%) and lower insertion loss (5dB) even without a anti reflection coating. During the course of the project related areas of interest in device research has			
20. DISTRIBUTION / AVAILABILITY OF ABSTRACT <input type="checkbox"/> UNCLASSIFIED/UNLIMITED <input type="checkbox"/> SAME AS RPT. <input type="checkbox"/> DTIC USERS		21. ABSTRACT SECURITY CLASSIFICATION Unclassified	
22a. NAME OF RESPONSIBLE INDIVIDUAL		22b. TELEPHONE (Include Area Code)	22c. OFFICE SYMBOL

UNCLASSIFIED

SECURITY CLASSIFICATION OF THIS PAGE

Box 19, continued:

been discovered. Among these, electro-optic polymers for high speed modulators and integrated circuit probes have received the most attention so far. A new guest/host system of purely commercially available chemicals had been developed and basic material characteristics in the 1 to 100 GHz are being measured. A more recent research effort that has come out of this project is the investigation of the use of the plasma effect in semiconductors for modelocking of solid state lasers. (C) W

UNCLASSIFIED

SECURITY CLASSIFICATION OF THIS PAGE

Contents

Executive summary.....	3
Introduction.....	4
Design, development and testing of the silicon light modulator.....	4
The silicon modulator in an all fiber system.....	6
Optical powering of silicon integrated circuits.....	10
Electro-optic polymers for high speed modulators and integrated circuit probes.....	10
Modelocked based on the plasma effect.....	18
Publications.....	18
List of scientific personnel.....	18

Appendix 1 B.R. Hemenway, O. Solgaard, D.M. Bloom, "All-silicon integrated optical modulator for 1.3 μ m fiber-optic interconnects", Appl. Phys. Lett. 55 (4), 24 July 1989.

Appendix 2 B.R. Hemenway, O. Solgaard, A. A. Godil, D.M. Bloom, "A Polarization-independent Silicon Light Intensity Modulator for 1.32 μ m Fiber Optics", to be published.

Appendix 3 O. Solgaard,, A. A. Godil, B. R. Hemenway, D. M. Bloom, "Pigtailed single mode fiber optic light modulator in silicon", to be published.



Accession For	
NTIS GRA&I	<input checked="" type="checkbox"/>
DTIC TAB	<input type="checkbox"/>
Unannounced	<input type="checkbox"/>
Justification	
By _____	
Distribution/	
Availability Codes	
Dist	Avail and/or Special
A-1	

List of illustrations

Figure 1	Scanning electron micrograph of first generation silicon modulator.	5
Figure 2	Schematic cross section of silicon modulator with fiber optic pigtail.	7
Figure 3	Photograph of silicon modulator/pigtail assembly.	8
Figure 4	Polarization independent fiber optical system utilizing the silicon modulator.	9
Figure 5	Probing of voltages on multi-chip modules using organic electro-optic films.	12
Figure 6	Formulas for the two optically nonlinear molecules, and PMMA and PCMA hosts.	14
Figure 7	Structure for measuring the poling induced birefringence and EO coefficient of the guest/host system.	15
Figure 8	Optical set up for measurement of the effective EO coefficient when the poled film is used as a probe.	16
Figure 9	Ring oscillator fixture for measurement of the dielectric constant and loss tangent in the polymer films at frequencies in the 1 to 100 GHz range.	17

Executive summary

During the one year and three months that the project on the "Development of an All Silicon Integrated Optical Modulator for High Speed Data Communications and Sensor Applications" has been running, the goals for the project have all been met. The first generation silicon light intensity modulator had a modulation depth of up to 30 % in a bandwidth up to 200 MHz. In accordance with the intents of the project, the modulator occupied a small surface area and is fabricated using standard silicon technology, making the modulator suitable for integration with silicon integrated circuits. The second generation of the modulator had several refinements, among which the push-pull design proved to be the most worthwhile, giving a doubling of the modulation depth. In the design of the modulator special emphasis was put on easy interfacing with fiber optics, and it was demonstrated that the modulator could not only simply and inexpensively be directly coupled to single mode optical fibers (pigtailed), but that the direct coupling of the modulators was more effective and led to a higher modulation index (24 %) and lower insertion loss (5 dB) even without an anti reflection coating. During the course of the project related areas of interest in device research have been discovered. Among these, electro-optic polymers for high speed modulators and integrated circuit probes have received the most attention so far. A new guest/host system of purely commercially available chemicals has been developed and basic material characteristics in the 1 to 100 GHz are being measured. A more recent research effort that has come out of this project is the investigation of the use of the plasma effect in semiconductors for modelocking of solid state lasers.

Introduction.

Due to large bandwidth and noise immunity, fiber optics has long been the choice for long distance communication, and its use in local area networks is steadily increasing. Correspondingly, there is an increasing need for a simple and inexpensive interface between fiber optics and silicon integrated circuits, the most widely used medium for computation and data processing. The motivation for the work on the silicon light intensity modulator is to develop such an interface. Specifically the goal was to develop a light modulator with the following characteristics:

- The fabrication of the modulator should be compatible with silicon integrated circuit technology. This is important because it allows the integration of electrical circuitry and the fiber optical interface on the same silicon chip without excessive extra processing cost.
- The modulator should be small. If the area taken up by the modulator is too large, the amount of circuitry that can be integrated with the modulator is limited.
- The fiber/modulator interface should be simple and have low loss. The advantages of integrating the modulator with electrical circuits would be reduced if the coupling of the modulator to the fiber has to be done by lenses or if the coupling has to conform with very stringent alignment tolerances.

Beside the original goals, several new areas of research has been identified through the work that has been done on this project. The most important of these is the investigation of the potential of polymer films for electro-optic modulators and internal sampling of silicon integrated circuits and multi-chip modules. Recently we also begun looking at the possibility of using the plasma effect in semiconductors, which is the physical effect that the silicon modulator is based on, for mode locking of solid state lasers.

Design, development and testing of the silicon modulator.

Within the one year and three months that the silicon modulator program has been running, a silicon modulator with the desired characteristics has been developed. Design, development of fabrication methods, based on a silicon bipolar transistor process, manufacturing and test of the first generation modulator was finished by the end of 1988.

The fabrication took place at the Center for Integrated Systems at Stanford University, using only standard silicon integrated circuits technology. Key points in the process development was the plasma etched, high aspect ratio isolating trenches, and the phase delay oxide of correct thickness. A scanning electron micrograph of the first generation modulator is shown in figure 1.

In the testing of the first generation modulator, lens coupling was used to interface the modulator with the optical fiber. This allowed testing of a wide range of modulator sizes. The smaller devices had a 10 % modulation index in a 200 Mhz bandwidth. At lower frequency the modulation depth was up to 30 %.

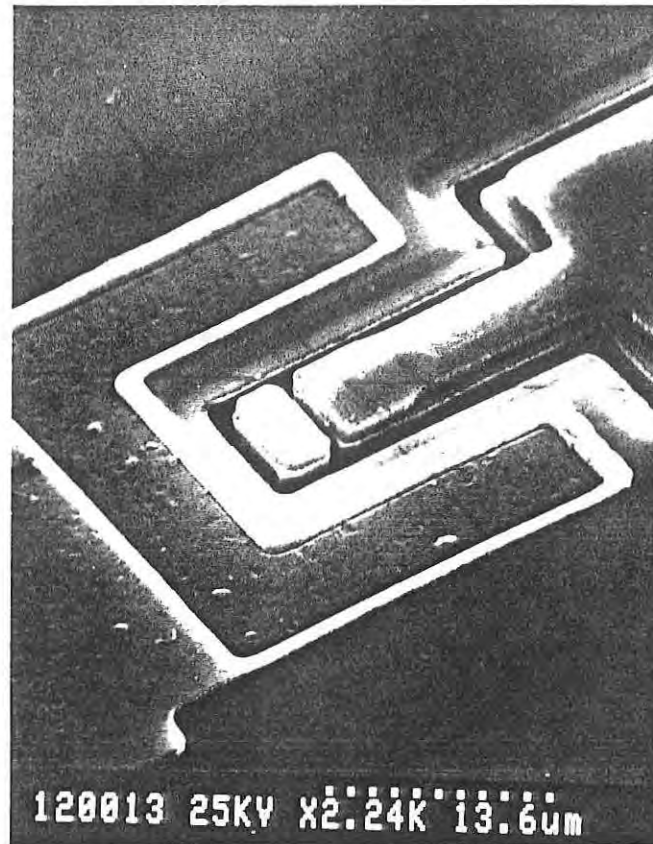


Figure 1

Scanning Electron Micrograph showing the geometry of the first generation silicon modulator. The free standing, passive part of the modulator is separated from the active part by a high aspect ratio trench. The electrical contact to the buried layer surrounds the modulator on three sides.

The design, development and test results of the first generation was reported in *Applied Physics Letters* in July of 1989 (appendix 1).

In the second generation of the modulator, several refinements were tried. Most importantly the new device was configured as a "push-pull" modulator. While the first generation had a passive side that provided the reference for the phase modulated side, the second generation had two active sides driven out of phase, thereby doubling the modulation efficiency. The tests on the second generation modulators showed the expected 3 dB increase in modulation depth. This result has been submitted for publication in *Photonics Technology Letters* (appendix 2).

The fabrication of the second generation modulator was similar to the original process, with two exceptions. First the buried layer was designed to have an increased doping level. This makes it possible to increase the charge density in the intrinsic region of the device. Increased charge density leads to higher modulation depth and higher bandwidth through reduced carrier lifetime. Unfortunately, technological problems hindered us in obtaining the desired doping levels, and we did not achieve the corresponding increase in modulation depth and frequency response.

We also tried to increase the reflectivity of the metallization by incorporating a titanium diffusion barrier. This however did not lead to a significant improvement.

The silicon modulator in an all fiber optic system.

To make the modulator practical, we needed to demonstrate its use in an all fiber system with no bulk optical components. To this end we took advantage of the small area and horizontal structure of the silicon modulator to directly couple a fiber pigtail to it. A schematic of the modulator with a pigtail is shown in figure 2. The silicon chip is mounted face down on the backside of the chip holder, and is wire bonded to through a hole in the holder. The package is filled with epoxy to give support during the thinning of the silicon chip. Thinning is necessary because the modulator does not have a waveguide, so the total propagation of the light before it is reflected back into the fiber must be less than the Rayleigh length, which in silicon is 260 μm for a single mode fiber at 1.3 μm .

The single mode fiber is glued in a glass capillary which is then polished to produce a clean fiber end. This assembly is then positioned over the modulator and glued with UV-epoxy while the modulation signal is monitored for easy alignment. A photograph of the finished modulator package is shown in figure 3.

The total fiber optical system is shown in figure 4. The source is a 1.3 μm distributed feedback laser with 3 mW output power, but even a light emitting diode or super luminescent diode would have a sufficiently narrow linewidth to be used in this system. The fiber coupler is a passive, polarization insensitive 3 dB coupler. The receiver is a InGaAs diode integrated with an amplifier.

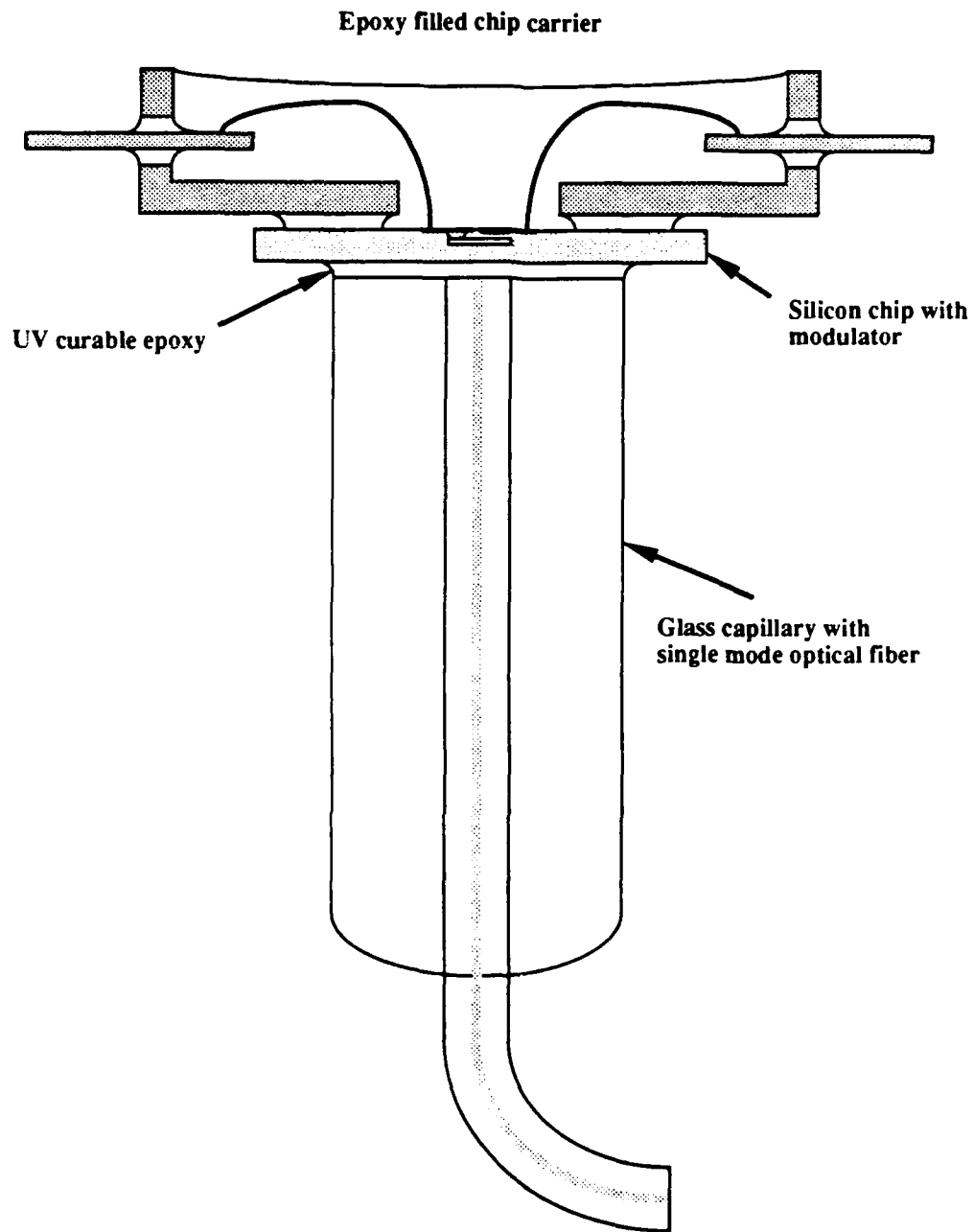


Figure 2

Schematic cross section of the silicon modulator with fiber optic pigtail. The silicon chip is mounted on the back of the chip carrier as shown. The capillary with the fiber is then positioned and glued while the signal is monitored.

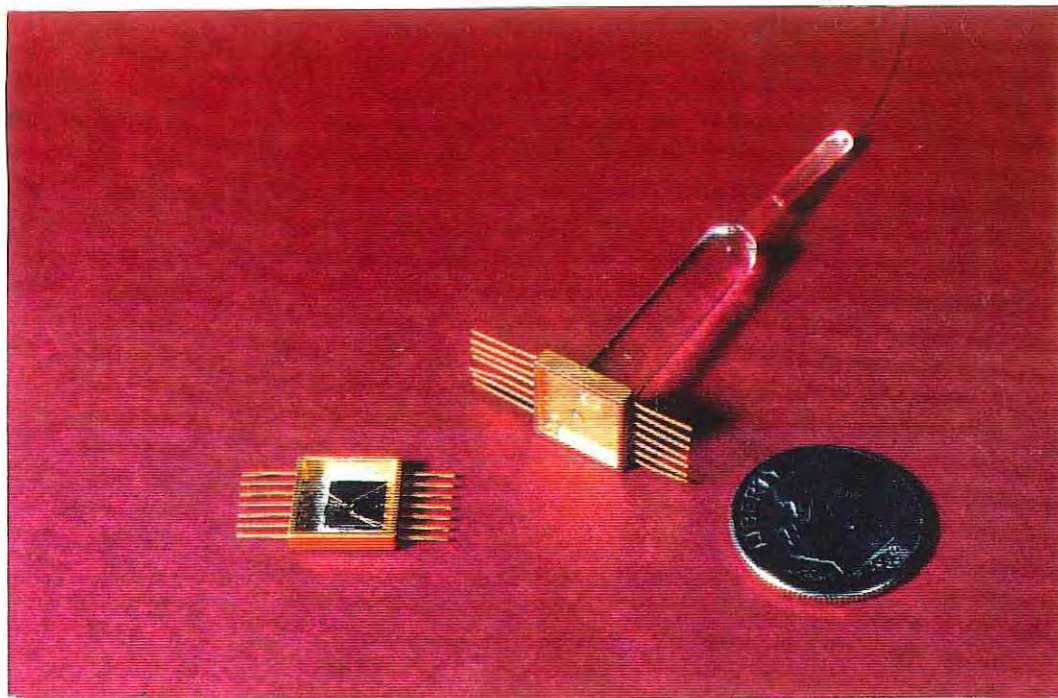


Figure 3 Photograph showing the package of the pigtailed modulator. The glass capillary with the fiber is glued directly to the back of the thinned silicon chip, which again is glued to the back of the chip holder. The bond wires to the silicon modulator goes through a hole in the chip carrier. For comparison, a modulator chip mounted in the standard fashion in the chip carrier is shown.

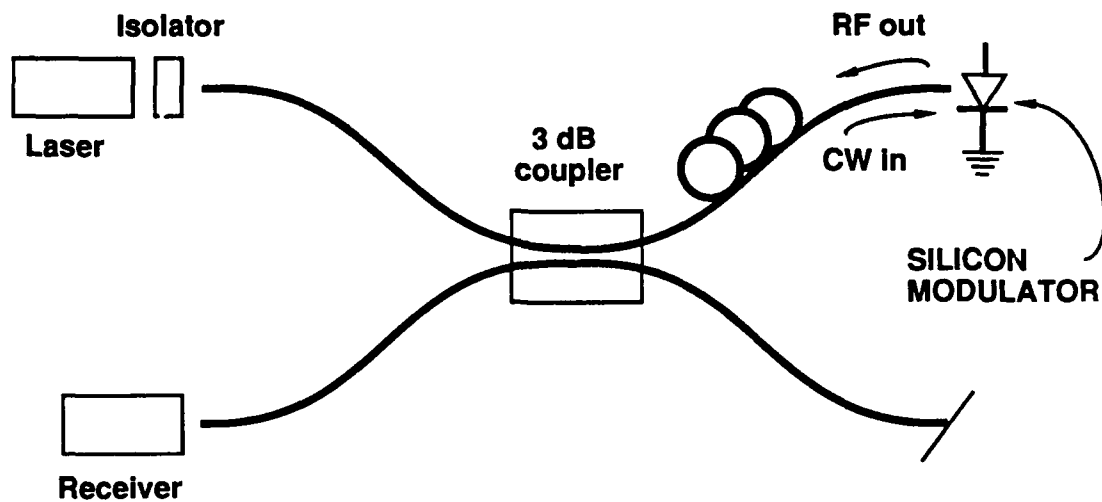


Figure 4

The silicon light modulator in an all fiber optic system. The 3 dB coupler, the receiver and the modulator itself have no polarization dependency, making the overall system polarization independent. Another silicon modulator could be coupled to the terminated port of the 3 dB coupler.

One greatly advantageous characteristic of the all fiber system is the fact that its polarization independent. The plasma effect is not dependent on the polarization state of the light. By using a polarization independent 3 dB power splitter, the overall system becomes polarization insensitive. This is important in a fiber system since the polarization state tend to vary with fiber stress and temperature.

The modulator with the pigtail is of the first generation design, but because of the direct fiber to modulator coupling, the measured modulation depth was higher, 24 % in a 60 MHz bandwidth with 5 dB insertion loss.

The pigtailed modulator does not have an AR coating at the fiber/silicon interface. With an AR coating the modulation depth should theoretically be twice as high as the 24 % we measure. As for the push-pull modulator, the results on the pigtailed silicon modulator has been submitted for publication in *Photonics Technology Letters* (appendix 3).

Optical powering of silicon integrated circuits.

The idea of optically powered silicon sensors with fiber-optic telemetry was investigated. This approach offers all the advantages of fiber-optic sensors in addition to a mature silicon sensor technology. The silicon optical modulator could be integrated with a sensor chip. The output of the sensor chip would drive the modulator and encode the data optically on the butt-coupled fiber. Electrical power to the sensor chip and the modulator could be provided by a photo-voltaic cell also integrated on the chip. To power to the photo-voltaic cell, a GaAs/AlGaAs laser at 800 nm would be used. The electrical power requirement is about 60 mW at 5 VDC. With a expected conversion efficiency of 40% this would require about 150 mW of pump light. To produce 5 volts, seven cells need to be connected in series since. Connecting cells in series requires that the cells be isolated with 30 μ m deep trenches. This kind of trench technology is possible in silicon, but keeping in mind the overall theme of our research group, we think our efforts would be better utilized looking at more novel concepts. However, we still feel that the idea of optically powered silicon sensors is feasible and very practical for commercial applications.

Electro-optic polymers for high speed modulators and integrated circuit probes.

An investigation of the use of organic electro-optic (OEO) materials in very high-speed optical modulators and sensors was begun in June of 1989. This work is motivated by the potential of OEO materials to extend the bandwidth of certain types of electro-optic devices to 100 GHz or more. The expected increase in bandwidth is based mainly on the projection that the dielectric constants of the OEO materials will remain near their low frequency values, which are typically between 3 and 5, throughout the radio frequency range. Such a low dielectric constant would result in a much smaller velocity mismatch between the radio frequency electrical drive signal and the optical beam in travelling wave modulators made using OEO materials rather than with the conventional LiNbO₃ technology. By contrast, LiNbO₃ has a low frequency dielectric constant on the order of 50. Another important attribute of OEO materials is that their electro-optic coefficients are also expected to remain roughly constant from low frequencies to well beyond 100 GHz. This expectation is supported by the fact that values of X_2 derived

from second harmonic generation measurements are of the same order as X_2 values derived from low frequency electro-optic modulator measurements. In addition, the necessary processing steps, such as poling, needed to produce a permanent electro-optic effect in the non-linear optical organic media are compatible with Si and GaAs circuitry making possible the fabrication of active integrated optical structures directly on the semiconductor drive circuitry.

The low dielectric constant and process compatibility with semiconductor circuits may also make possible the extension of optical probing techniques to electrical circuits fabricated on non-electrooptical materials or to hybrid structures such as multi-chip modules where access to the semiconductor substrates is blocked by the ceramic support structure. Many probing geometries are possible. In the configuration shown in figure 5, a poled OEO film, mounted on a transparent substrate, is held in contact with a Silicon chip in a multi-chip module.

The OEO film is thicker than the interelectrode spacing ensuring that most of the fringing fields, which are the fields that modulate the film's refractive index, are contained within the OEO layer. Two optical probe beams are retroreflected off of metalized portions of the electrical circuit, and pass through the OEO film twice. One beam probes an active portion of the circuit while the second reflects off of a ground line and serves as a reference. By measuring the phase difference between the two beams, the voltage on the active line can be determined. The low dielectric constant of the OEO film should load the electrical circuit only slightly and certainly much less than would a LiNbO_3 probe.

Before OEO materials can be used reliably in such applications, their high frequency operating parameters, such as electro-optic coefficients, dielectric constants, and loss tangents, must be determined. The initial OEO work under this contract has therefore centered on developing techniques for measuring these basic material parameters.

A straightforward method for measuring the electro-optic coefficients at high frequencies is to fabricate an OEO layer on a GaAs substrate supporting a high frequency coplanar waveguide (CPW). The existing CPW active probes and the optical sampling test bed could then be used to drive the CPW and probe it from the GaAs side to determine the voltage at a particular location on the CPW. Probing the OEO layer on the other side of the CPW would yield the phase change induced by the voltage in the OEO layer and consequently the electro-optic coefficient at the frequency at which the CPW was driven. To facilitate the use of the CPW active probes, access holes through the polymer layer to the underlying CPW must be created.

Laser ablation has been used to etch holes in a variety of materials. Using the Ar-F excimer laser (Cymer Lasers) located in Stanford's Center for Integrated Systems facility we have demonstrated laser ablation of two organic materials chosen to simulate existing OEO materials. Some of the current OEO materials are pendant side-chain polymers which have backbones similar to Poly(methyl methacrylate) (PMMA). Other researchers have presented data on fully cross-linked OEO structures. PMMA and Norland 63 (a fully cross-linking uv curable coating) were therefore chosen as the polymers to be tested. For the 193 nm Ar-F line and pulse fluences of 180 $\text{mJ}/\text{cm}^2/\text{pulse}$, ablation rates of $0.56 \mu\text{m}/\text{J}/\text{cm}^2$ and $0.64 \mu\text{m}/\text{J}/\text{cm}^2$ were measured for PMMA and Norland 63 respectively. Ablation was performed using the focussed attenuated beam and also by imaging a pattern on a chrome-on-glass mask onto the polymer films with the uv radiation. Both techniques worked well, demonstrating the effectiveness of laser ablation in creating the needed via holes.

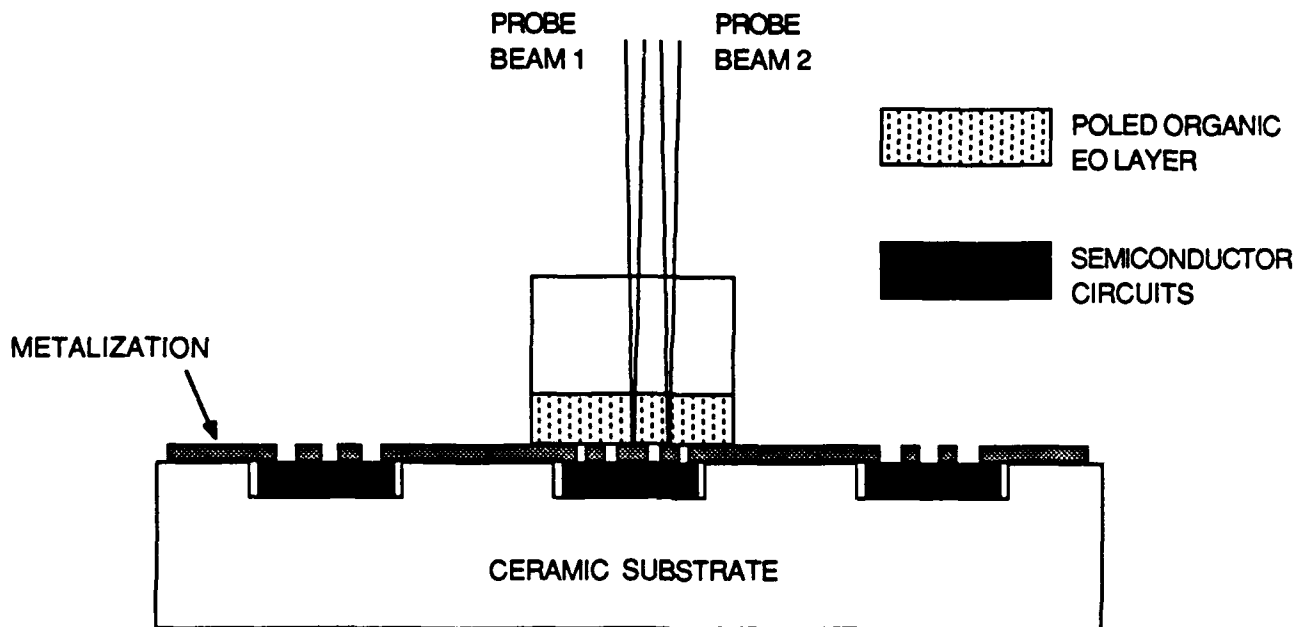


Figure 5

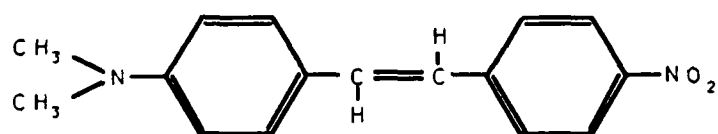
The optical probing of electrical circuits in multi-chip modules could be accomplished by measuring the refractive index change in an organic electro-optic film held in contact with the circuit under test. In the configuration shown above, optical probe beam 1 retroreflects off of an active portion of the circuit while probe beam 2 retroreflects off of a ground line and serves as a reference. By measuring the phase difference between the two beams the voltage on the active line relative to ground can be determined.

None of the reported side-chain or cross-linked OEO materials are yet available commercially. These materials can support high percentages of NLO moieties and can retain a large fraction of the poling induced electro-optic effects for over a year or more. For initial optical probing and modulator research these characteristics are desirable but not essential. In order to carry out proof-of-principle experiments we have developed a guest/host system, and a compatible poling process for it, composed of commercially available materials. Consideration was also given to formulating a solution from which thin films of the guest/host material could be spun coated. A large number of mixtures were tested. The mixtures consisted of either 4-dimethylamino-4'-nitrostilbene (DANS) [Kodak], or Disperse Red 1 (DR1) [Aldrich] as the electro-optic guests; PMMA, poly(cyclohexyl methacrylate) (PCMA), polystyrene, and polycarbonate [all from Scientific Polymer Products] as the hosts; and over ten solvents including Acetone, AZ photoresist thinner, Chlorobenzene, Chloroform, Cyclohexanone, 1,2-dichloroethane, DMA, DMF, THF, Toluene, and Xylenes. Molecular formulas for the two electro-optic guests, PMMA, and PCMA are shown in figure 6. Most OEO guest/host systems reported in the literature have used PMMA as the host. PCMA has been used effectively in polymer blend systems so we included it in our study. We have found 10% by weight DR1 in PCMA in a solution of 0.25 grams of solids (DR1 + PCMA) per ml of cyclohexanone to be the best overall system we have formulated so far. DR1 is, in general, much more soluble than DANS allowing more concentrated solutions to be made. More concentrated solutions produce thicker films which are advantageous in optical probing geometries. To the best of our knowledge, this guest/host system has not been reported in the literature. Smooth films, 3 μm thick, were produced from this solution by spinning at 2000 rpm. It should be possible to produce much thicker films using multiple applications.

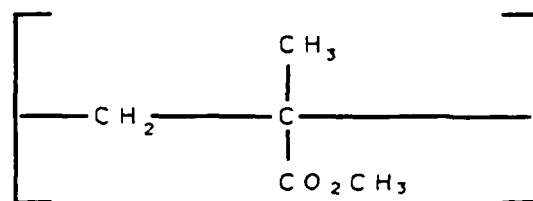
A real-time ellipsometer/poling station has been developed by researchers in Stanford's Material Science department. This facility, located in the Keck building, was used to characterize the poling induced birefringence in our guest/host material as a function of temperature and poling field. The structure used in this test, shown in figure 7, was fabricated in the Ginzton Microstructures facility. Results from these measurements indicate that a poling temperature of approximately 85 Deg. C. is near optimum for all poling fields.

A poling fixture was built in order to carry out the poling in a conventional oven located in Ginzton Laboratory. The fixture was designed to support the test structure and electrical leads both during poling and during the subsequent optical probing measurements. The following poling sequence was used: 1) the sample was heated to near 85 Deg. C.; 2) a field of 85 V/ μm was then applied for roughly 30 sec before the cooling cycle was begun; 3) the sample was slowly cooled back to room temperature with the field maintained at 85 V/ μm ; 4) after cooling back to room temperature, which froze in the induced alignment, the poling field was reduced to zero.

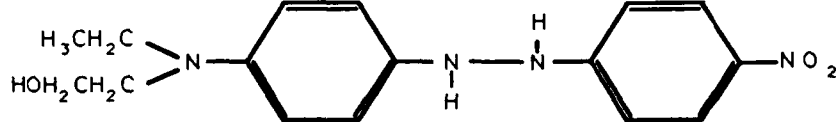
To determine the electro-optic coefficient of the poled film when used in a configuration similar to that which will be used in the actual optical probing test bed, the setup shown in figure 8 was built. Due to the large capacitance of the test structure and the high resistance of the transparent Indium-Tin-Oxide electrode, electro-optic measurements could not be taken at frequencies above a few KHz. At 1 KHz, r_{13} was measured to be approximately 2 pm/V and remained near that value for over a week (fairly stable for a guest/host system). These levels of electro-optic performance and stability should be more than enough for use in high speed measurements using GaAs substrates.



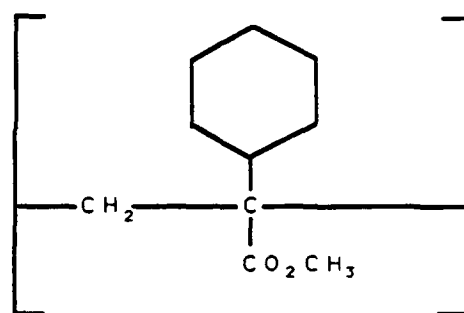
4-dimethylamino-4'-nitrostilbene



Poly(methyl methacrylate)



Disperse Red 1



Poly(cyclohexyl methacrylate)

Figure 6 Schematic diagrams of the two electro-optic organic molecules and two of organic host materials used in the guest/host studies. Disperse Red 1 is available from Aldrich, 4-dimethylamino-4'-nitrostilbene is available from Kodak, and both hosts are available from Scientific Polymer Products.

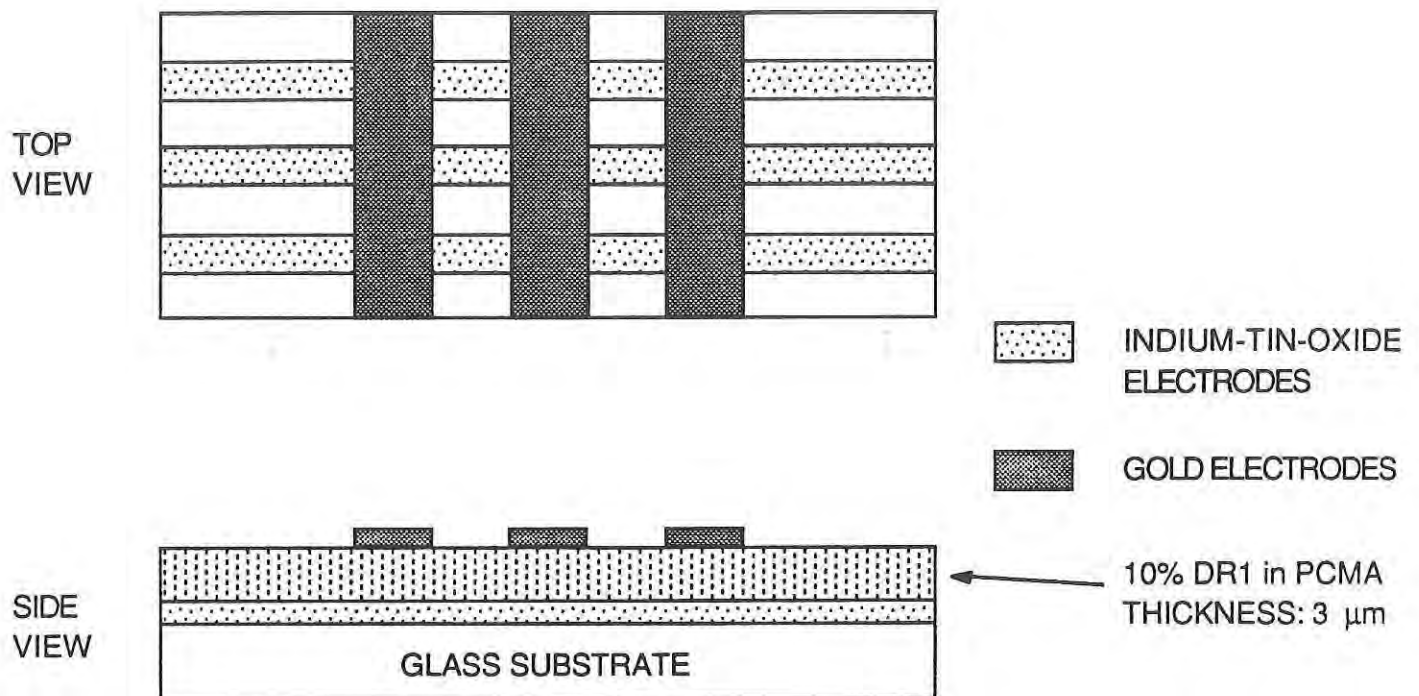


Figure 7 Schematic diagram of the test structure used for the measurement of the poling induced birefringence and the poling induced electro-optic coefficient. The transparent indium-tin-oxide (ITO) electrodes facilitate the optical measurements of the poled region between the gold and ITO electrodes. The array of polable cells allows a variety of poling processes to be evaluated using the same structure.

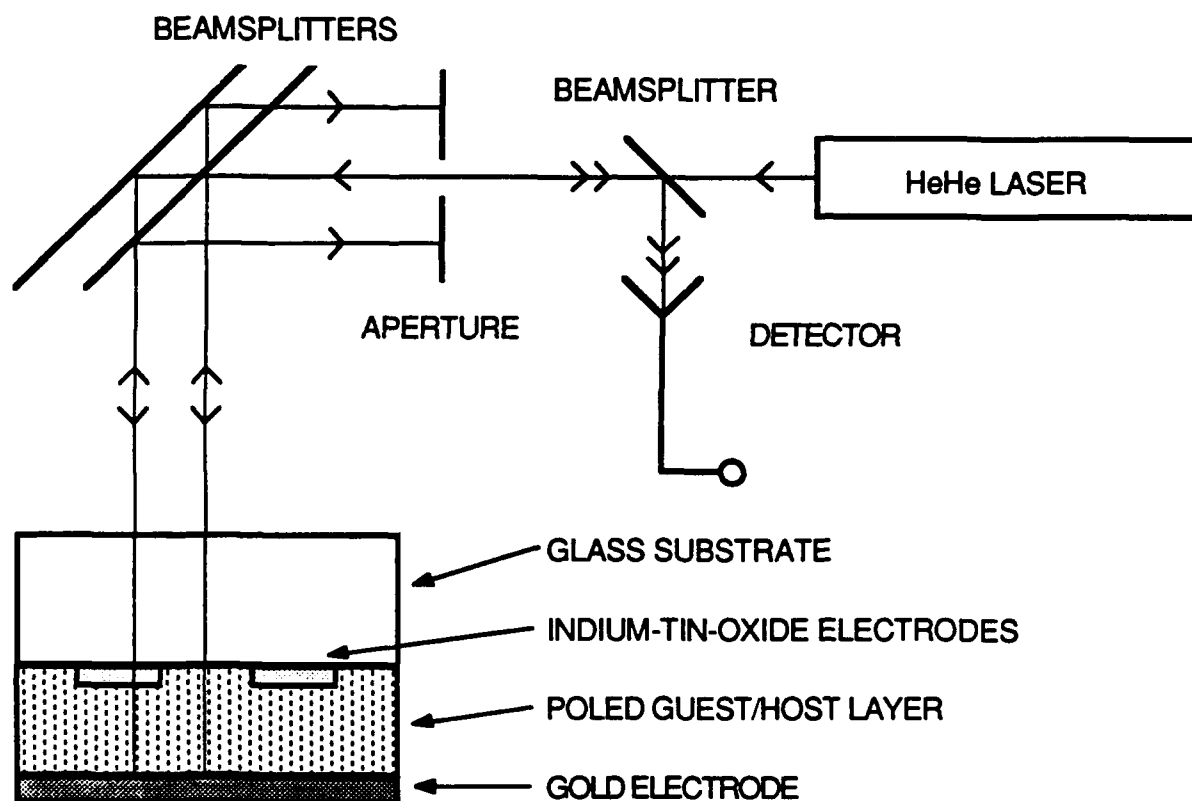
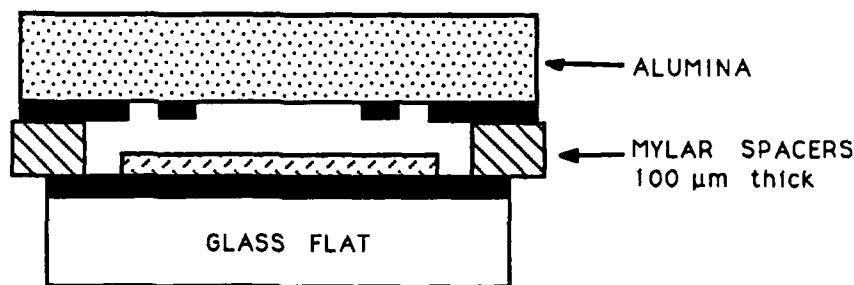




Figure 8 Schematic diagram of the electro-optic measurement/optical probing simulation setup. The pair of beamsplitters creates two beams, one which passes through a portion of the film having electrodes on both sides while the other beam passes through an unmodulated area and serves as a reference. By measuring the interference between the two beams and the intensity corresponding to a π phase shift between the beams, the electro-optic coefficient can be determined.

**SIDE
VIEW**



-  METAL (1-5 μm thick)
-  EO POLYMER, OR BUFFER LAYER (3-10 μm thick)

**TOP
VIEW**

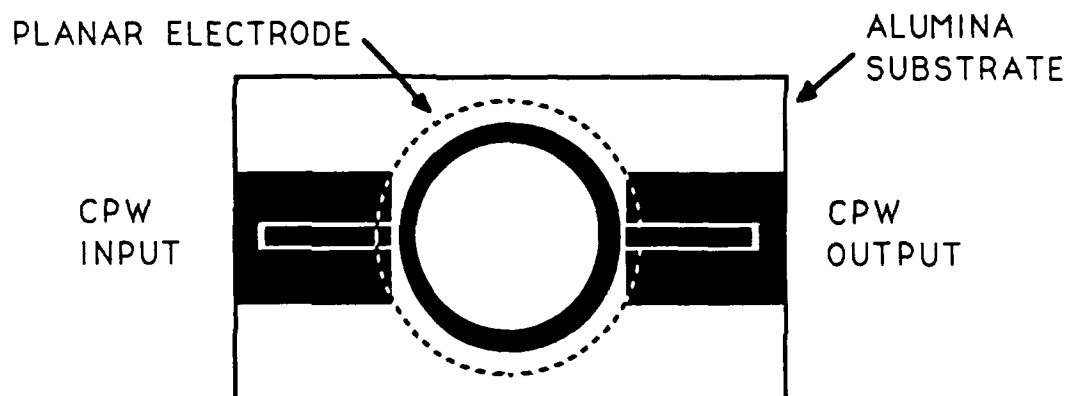


Figure 9 Schematic diagrams of the ring resonator fixture that will be used to measure the dielectric constants of thin polymer films at frequencies beyond 1 GHz. The two coplanar waveguides (CPW) are lightly coupled to the microstrip ring resonator and act as input/output ports. By measuring the shift in resonant frequencies due to the presence of a film deposited on the ground plane (relative to the resonant frequencies measured when the ground plane is uncoated) the dielectric constant of the film material can be determined.

Efforts have also been made to develop a fixture for measuring the dielectric constant of OEO films at frequencies above 1 GHz. A schematic diagram of the fixture is shown in figure 9. The measurement technique is based on the ring resonator design. In our fixture, two CPWs are lightly coupled to the ring and act as input/output ports. A planar electrode is held a fixed distance from the ring and serves as the ground plane for the microstrip ring resonator. By measuring the shift in resonant frequencies due to the presence of a film deposited on the ground plane (relative to the resonant frequencies measured when the ground plane is uncoated) the dielectric constant of the film material can be determined at the resonant frequencies. It may also be possible to determine the loss tangent of the material by measuring the change in the resonator Q. A scaled prototype of this fixture was built using epoxy board and the frequency shifts due to the presence of a thin teflon film were easily measured. A properly dimensioned fixture, made from high quality alumina and 1/10 wave optical flats is now being fabricated.

Once the high frequency values of the dielectric constant, and perhaps the loss tangent, of the guest/host system have been measured, the optical probing experiments using CPW electrodes on GaAs substrates will begin.

Mode locker based on the plasma effect.

Currently we are investigating the idea of building a plasma effect phase modulator to mode-lock a 1.06 μm solid state laser. This wavelength is slightly above the bandgap of silicon and therefore GaAs/AlGaAs material system was chosen for initial design conception. In GaAs in addition to the plasma effect, the band-filling effect also contributes considerably to the index change. With GaAs/AlGaAs technology a dielectric mirror can also be grown along with the modulator. This could then conveniently replace one of the mirrors of the laser cavity to produce a mode-locked laser.

Publications.

- [1] B.R. Hemenway, O. Solgaard, D.M. Bloom, "All-silicon integrated optical modulator for 1.3 μm fiber-optic interconnects", Appl. Phys. Lett. 55 (4), 24 July 1989.
- [2] B.R. Hemenway, O. Solgaard, A. A. Godil, D.M. Bloom, "A Polarization-independent Silicon Light Intensity Modulator for 1.32 μm Fiber Optics", to be published.
- [3] O. Solgaard, A. A. Godil, B. R. Hemenway, D. M. Bloom, "Pigtailed single mode fiber optic light modulator in silicon", to be published.

Participating scientific personnel.

In addition to the principal investigator, Dr. D.M. Bloom, the following graduate students have been working on the silicon modulator project: B.R. Hemenway, O. Solgaard, A.A. Godil and J.I. Thackara. B. R. Hemenway expects to finish his doctoral degree in Applied Physics by June 1990.

All-silicon integrated optical modulator for 1.3 μm fiber-optic interconnects

B. R. Hemenway, O. Solgaard, and D. M. Bloom

Edward L. Ginzton Laboratory, Stanford University, Stanford, California 94305-4085

(Received 27 February 1989; accepted for publication 15 May 1989)

We report an all-silicon fiber-optic light modulator which relies on free-carrier optical dispersion and mode filtering in single-mode fibers. Greater than 10% peak-to-peak intensity modulation over a 200 MHz bandwidth for 10 mA rf current modulation at 1.3 μm wavelength is demonstrated.

Systems based on silicon technology could benefit greatly by a fully integrated interface with optical fibers both for interconnects and local area networks. Unfortunately, silicon integrated circuits (ICs) have not been used for active optical elements in fiber communications systems near 1.3–1.55 μm because silicon is neither electro-optic nor efficient at absorbing or emitting light at these wavelengths. However, free-carrier dispersion has been used as the basis for sensitive optical probes of charge density in ICs,¹ for phase modulation of optical beams in forward-injected InP² and silicon³ waveguide modulators, and as the dominant mechanism in depletion-charge waveguide modulators.⁴

Here we report a reflection-type integrated silicon optical modulator (SIMOD) that modulates the coupling of light to a single-mode optical fiber positioned normal to the plane of the substrate. The SIMOD uses free-carrier dispersion to diffract the optical beam. The silicon bipolar device is compatible with other silicon technology and its small size allows for high levels of integration and parallelism. It achieves 10% peak-to-peak intensity modulation at 1.3 μm over 200 MHz modulation bandwidth using 10 mA dc bias and 10 mA rms rf current.

The SIMOD uses free-carrier dispersion to spatially modulate the phase of an optical beam. Subsequent phase-modulation to amplitude-modulation conversion occurs by mode selection in the single-mode fiber. The light output of a single-mode fiber is imaged into the active region of the modulator. In the device, one-half of the beam is phase delayed relative to the other half. The phase delay consists of two parts, a static delay of $\lambda/4$ and a separate, modulated delay due to free-carrier injection. The spatially modulated beam is coupled back into the optical fiber whose propagation properties strip the beam of new components of odd symmetry and high mode number. In effect, the optical path difference and the modulated free-carrier density diffract the optical beam and excite a continuum of nonpropagating radiation modes in the fiber. This results in intensity modulation in the fundamental optical component coupled to the fiber core. This effect is similar to the diffraction that occurs in Y-type mode-coupling waveguide junctions and Mach-Zender switches.⁵ The static delay or "bias" maximizes the sensitivity of the intensity modulation to the phase modulation and also maximizes its linearity. The static phase delay is chosen so that free-carrier absorption enhances the net intensity modulation. The operation of the device is polarization independent and wavelength insensitive and hence

the device can also be used with high-radiance light-emitting diodes (LEDs). The geometry allows the fiber to be butt-coupled normal to the plane of the modulator, reducing the optical complexity of the interconnect by eliminating optical elements. The present results, however, use lenses to image the fiber into the device rather than butt coupling.

The active component of the device is a $3 \times 6 \mu\text{m}^2$ integrated silicon *pin* diode operating under forward bias (Fig. 1). The vertical diode is defined by epitaxial layers and a boron implant. Two *n*-type silicon layers each 6 μm thick are grown on an *n*⁻ substrate: the first layer grown is doped at $2 \times 10^{18} \text{ cm}^{-3}$ and the second at $2 \times 10^{14} \text{ cm}^{-3}$. A deep *n*⁻ contact is diffused followed by a thermal oxidation yielding an oxide 960 Å thick. This oxide forms part of the static optical phase delay region which aids the diffraction effect. A carrier isolation trench 5 μm deep and 1.5 μm wide is then dry etched. Boron, implanted at low energy, forms the *p*⁺/*n*⁻ junction. Another short oxidation activates the implant, passivates the trench surface, and completes the phase delay oxide. Finally, aluminum contacts are made, and the wafer is annealed and polished. A typical device occupies an area of $28 \times 34 \mu\text{m}^2$, exclusive of bond pads.

After dopant outdiffusion, the intrinsic region has narrowed to 3.5 μm . This width essentially sets the achievable modulation depth which is controlled by the diffusion capacitance associated with carrier injection into the *i* region. Modulation speed is determined by the rate at which carriers can be injected and removed. Abrupt junctions are used to ensure high carrier gradients and thus efficient carrier injection and removal especially under rf modulation since the carrier modulation is most efficient at the intrinsic region boundaries.⁶ By operating at injection levels above about $5 \times 10^{17} \text{ cm}^{-3}$, Auger mechanisms dominate the recombina-

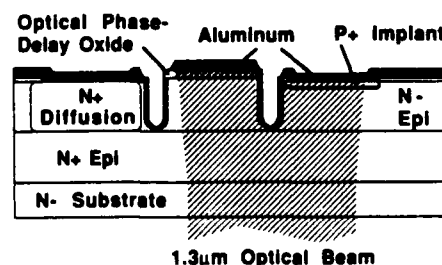


FIG. 1. Schematic cross section of an integrated silicon optical modulator shown with optical beam.

tion process, thereby increasing the frequency response of the device. This requires a current density of about 1×10^5 A/cm².

We demonstrate the operation of the silicon modulator in a simple fiber transmission experiment. A multimode 1.3 μ m cw InGaAsP laser beam passes through an optical isolator and is focused into a short length of step-index single-mode fiber having a normalized frequency of 2.1. An in-line fiber polarization controller is adjusted to provide a quarter-wave rotation in the polarization vector of the optical beam. The fiber output is imaged into the optical modulator. After reflection and modulation, the beam travels back along its original path and emerges at the input of the fiber in a polarization state orthogonal to that of the input laser beam. A polarizing beamsplitter then deflects the modulated beam into a wideband photodetector. Increased electrical current results in decreased coupling of the reflected light into the fiber. The sensitivity of the laser to optical feedback noise requires the use of an optical isolator with its polarizing elements. This arrangement, although not fundamental to the operation of the modulator, also increases the received optical power by 6 dB since power is not lost by polarization-insensitive directional couplers which might otherwise be used. However, the use of a high-radiance LED and elimination of the polarization maintaining elements would significantly reduce the complexity of the interconnect system.

The performance of the SIMOD was measured by placing the *pin* diode in series with a 47 Ω resistor for ease of driving with a 50 Ω source. The signal from the photodetector is amplified by 46 dB for display on an oscilloscope or spectrum analyzer. An eye diagram of the data transmission response of the SIMOD is shown in Fig. 2 for a 20 bit pseudorandom nonreturn-to-zero (NRZ) word at a data rate of 55 Mbit/s. The peak current is 26 mA with no dc bias. The swept frequency response of the modulator is shown in Fig. 3 where the different curves correspond to various rf current modulation conditions. In all cases, dc bias was 10 mA. Peak-to-peak modulation depths exceeding 35% are attained for sufficiently high levels of injection. At low to intermediate drive levels, the unequalized response is reasonably flat, showing a -3 dB bandwidth of 200 MHz at 10 mA rms

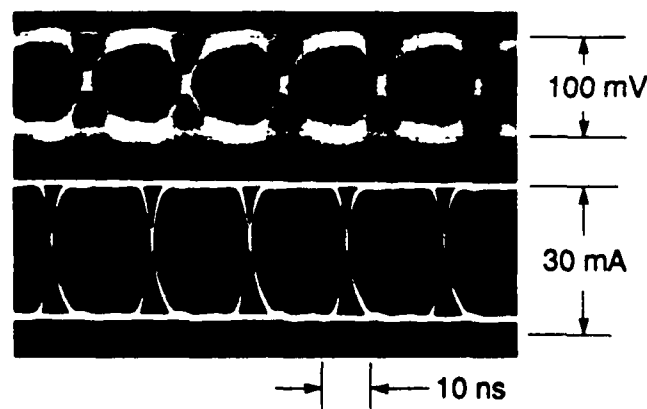


FIG. 2. Oscilloscope photograph of eye diagrams of a NRZ 55 Mbit/s pseudorandom word transmitted (bottom) and received (top).

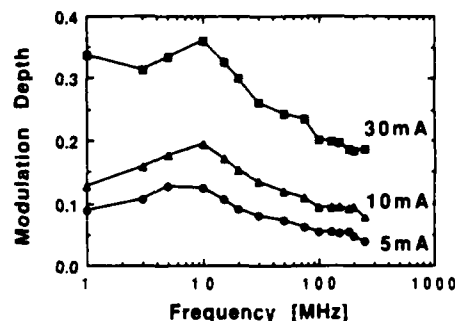


FIG. 3. Frequency response curves of the SIMOD for three rms rf current modulation conditions. Bias is 10 mA. The response at 10 mA exceeds 10% peak-to-peak modulation depth over a bandwidth of 200 MHz. At higher injection levels, the SIMOD achieves 35% modulation over limited bandwidth.

rf and 10 mA dc. In integrated form, the modulator can be driven by low-impedance sources similar to those used for driving low-threshold lasers under large signal modulation. However, higher speed can be expected by applying a reverse bias during the off portion of a transmitted digital signal to aid the removal of carriers.

The silicon optical modulator is a unique device that has several advantages over conventional optical intensity modulators. These include monolithic silicon compatibility and polarization-independent operation. The device also avoids several problems associated with integrated waveguide modulators, namely, that they use large areas, generally must be edge coupled, and cannot easily be integrated with large-scale silicon ICs. The ultimate performance of a SIMOD device for digital applications depends primarily on the current drive available and the modulation depth required to achieve a given signal to noise ratio over a specified bandwidth. For instance, many local-area communications systems and sensor systems do not require 100% intensity modulation. In these applications, the SIMOD can be optimized to trade off modulation bandwidth with modulation depth by adjusting the diode capacitance. The fabrication compatibility of the silicon optical modulator and its demonstrated performance suggest that it may be best suited to local area networks, fiber-to-the-home return links, interconnects, and sensor systems.

This work was supported by the Army Research Office under contract DAAL03-88-K-0120, the Joint Services Equipment Program under contract N00014-84-K-0327, and the Stanford University Center for Integrated Systems (CIS) Seed Research Program. The authors also wish to acknowledge computer modeling support donated by Technology Modeling Associates Inc., and valuable contributions by R. Swanson and the CIS technical staff.

¹B. R. Hemenway, H. K. Heinrich, J. H. Goll, Z. Xu, and D. M. Bloom, *Electron Device Lett.* **50**, 83 (1987).

²O. Mikami and H. Nakagome, *Electron. Lett.* **22**, 228 (1984).

³J. P. Lorenzo and R. A. Soref, *Appl. Phys. Lett.* **51**, 6 (1987).

⁴A. Alping, X. S. Wu, T. R. Hausken, and L. A. Coldren, *Appl. Phys. Lett.* **48**, 1243 (1986).

⁵W. K. Burns and A. F. Milton, *J. Quantum Electron.* **11**, 32 (1975).

⁶D. Leenov, *IEEE Trans. Electron Devices* **11**, 53 (1964).

A Polarization-Independent Silicon Light Intensity Modulator for 1.32 μm Fiber Optics

B. R. HEMENWAY, STUDENT MEMBER, IEEE, O. SOLGAARD, MEMBER, IEEE,
A. A. GODIL, AND D. M. BLOOM, SENIOR MEMBER, IEEE

The authors are with the
E. L. Ginzton Laboratory, Stanford University, Stanford, CA, 94305.

Abstract - We have developed an integrated silicon light intensity modulator based on polarization-independent free-carrier optical phase modulation and mode filtering in fibers. A novel push-pull complementary diode pair are used for a twofold increase in modulation depth over a single diode device. Operation is demonstrated at a wavelength of 1.32 μm .

INTRODUCTION

In a previous paper we described a new kind of all-silicon light intensity modulator based on free-carrier dispersion and the mode filtering properties of single mode fibers [1]. In that device, free carriers modulate the phase of one half of a $1.3\text{ }\mu\text{m}$ laser beam, generating field components of odd symmetry by coherent interference. Mode selection in a single-mode optical fiber strips all but the fundamental component for propagation, converting phase to amplitude modulation. The small-area silicon device employed a single forward-injected pin diode for the active modulation. An inactive phase-delay region was used to provide a reference phase for the interference effect. In this paper we describe an extension of this concept wherein two *pin* diodes, driven out of phase, are used for "push-pull" phase modulation. We show that the differential phase modulation leads to a twofold gain in modulation depth. Polarization independence is preserved.

OPERATION AND DESIGN

The silicon light modulator is a reflection-type device. A cw $1.32\text{ }\mu\text{m}$ multi-longitudinal mode laser beam is coupled to a step-index single-mode fiber whose output is imaged into the active area of the modulator (Fig. 1). There, the forward-biased pin diodes are charged and discharged so that each half of the beam undergoes separate carrier-induced phase modulation. When the phase in the delayed half of the beam is increased (by reducing the carrier density in it) more light couples to the lossy cladding modes and less to the core mode. Conversely, when the phase in the undelayed half is decreased (by increasing the

carrier density in it) less light couples to the cladding modes and more to the core mode. Thus, by steering current between the two diodes, the total phase delay between the two halves is increased by close to a factor two over the single-sided version. A 1-2 mA bias is applied to keep the recombination rates in the diodes within the more responsive Auger regime.

Although the actual field profiles of a weakly guiding step-index single-mode fiber are described by a combination of Bessel and modified Hankel functions, the fields can be approximated by simple gaussian functions to better than 1% [2]. Let the reflectorless distance between the diodes be $2b$, the distance to the outer edge of the reflector be a and w the beam radius (Fig. 2). Also, let the total phase delay between the two halves the optical beam be ϕ_0 (a bias) plus $\Delta\phi$ (due to carrier-induced phase modulation). The intensity coupled back into the fiber can be determined by taking the dot product of the fiber mode and the modulated reflected fields. The coupled power then is

$$I = \frac{1}{2} \left[\operatorname{erf} \left(\sqrt{2} \frac{a}{w} \right) - \operatorname{erf} \left(\sqrt{2} \frac{b}{w} \right) \right]^2 (1 + \cos(\phi_0 + \Delta\phi)).$$

We have ignored the small changes in phase and waist size induced by propagation. This is valid when the back coupling occurs at a beam waist or within the Raleigh range of the fiber (270 μm in silicon). By ignoring beam expansion in the above analysis, we neglect an effective coupling loss of 0.36 dB for a substrate thickness of 50 μm . The radiated power is coupled to cladding modes or stripped altogether within a few millimeters of fiber length [3]. To maximize the small-signal modulation efficiency of the device and minimize sensitivity to wavelength variations, $\partial I / \partial \phi_0$ is maximize and $\partial I / \partial \lambda$ is minimized. This occurs for the first order phase plate, $\phi_0 = \pi/2$. To meet this condition, a one-pass delay of 471 Å in the silicon is built in. We describe below how this is achieved. The beam is adjusted in size and position by external optical elements. The device is designed so that a

fiber coupled directly to the modulator also has nearly the optimum beam size. The experimental results of such a configuration are described separately [4].

The intensity modulation depth and device size are determined by the diode diffusion capacitances. Since the index perturbation is nearly linear with electron and hole density over a very broad range of concentrations [5,6], the integrated carrier density should be maximized. However, since high capacitance also limits speed, there is an inherent modulation depth / bandwidth tradeoff for the two-pass geometry. The exact relationship is not a simple one because the rf carrier modulation efficiency decreases with frequency. Not only does the impedance change, but at high frequencies carriers are modulated most efficiently only near the edges of the device where there is a large concentration gradient [7]. The frequency dependence is minimized by maintaining very abrupt doping concentration gradients. In this device, the intrinsic region is $3.5\text{ }\mu\text{m}$ thick at a doping level of $5 \times 10^{17}\text{ cm}^{-3}$. The area under each contact mirror is $32\text{ }\mu\text{m}^2$. This provides a 300 pF diode at 40 mA and 184 pF at 10 mA. Such diodes can be driven with circuits similar to those used for driving laser diodes and LEDs [8].

FABRICATION

The device is fabricated by growing a $10\text{ }\mu\text{m}$ layer of n^+ silicon on an n^- $\langle 100 \rangle$ substrate, used to minimize free carrier absorption. A second lightly doped layer initially $7.5\text{ }\mu\text{m}$ thick follows. After an n^+ plug is sunk to the buried layer, the wafer is oxidized. To form the phase bias step, the oxide is removed over one diode but not the other. A 2230 \AA thermal oxide is produced on the open diode while an additional 1250 \AA is produced over the covered diode. In the $\langle 100 \rangle$ orientation, 44% of this oxide consists of silicon

consumed during growth [9]. The covered diode then has 431\AA more silicon than the unprotected diode. An additional 40\AA or so is removed by steps later in the process producing a measured $454\pm 12\text{\AA}$ step. This is close to the 471\AA phase delay required for optimum modulation. Implantation of boron at $5\times 10^{15}\text{ cm}^{-2}$ and 50 keV complete the diodes. A $1\text{ }\mu\text{m}$ layer of aluminum (with 1% Si) is deposited, patterned and alloyed. Finally the wafer is polished and packaged for optical access. Unlike the devices described previously, these devices do not have a trench for carrier isolation. While this will lower the ultimate modulation depth, it reduces the scattering losses and simplifies fabrication. The carrier modulation achieved here demonstrates that a large percentage of carrier modulation occurs near the abrupt p+/n- junctions which are somewhat isolated from one another by the short ambipolar diffusion length of less than two microns and the high carrier gradients.

RESULTS

The push-pull effect is seen in Fig. 3. There a TTL-level digital word representing the sequence *A* beginning 00100110... is transmitted through a 2 m fiber. That sequence is applied to one diode alone (upper curve) and its inverse sequence, namely *A-bar* = 11011001... is applied to the other diode alone (lower curve). When data *A* is applied to one diode and *A-bar* to the other diode simultaneously, then there is approximately a 3 dB improvement in the amplitude response (middle curve). Furthermore, there is a negligible increase in the noise level which is limited by laser relative intensity noise. Although the bias conditions in the two diodes were adjusted to achieve the best response, a slight additional droop is present whose low frequency components can lead to increased pattern dependence in the transmitted signal. If one diode is more forward-biased than its neighbor

then the turn-on and -off times will be affected as will the optical phase response. The beam is also carefully positioned (within $0.2\text{ }\mu\text{m}$) so that the two halves contribute equally to the received signal.

Essentially a charge storage device, the silicon modulator exhibits a single pole response (Fig. 4) for both push-pull and single-sided operation. The upper curve is for a push-pull configuration with 13 dBm rf power applied through a hybrid junction so the signal appearing at the diode terminals are 180° out of phase. Bias is applied separately through bias tees. The lower curve corresponds to a 10 dBm rf signal applied directly to the narrow base diode. The average increase in the measured peak-to-peak modulation depth for the increase of 3 dBm in rf signal is a factor of 1.51. This agrees with the expected increase of $\sqrt{2}$ due solely to an increase of $\sqrt{2}/2$ in the peak current. The slight increase in this ratio below 10 MHz is expected due to competing thermo-optic contributions the index change. These are less pronounced in the two-diode design because of symmetry.

CONCLUSION

We have described the operation, fabrication and performance of a small-area silicon integrated light intensity modulator for $1.32\text{ }\mu\text{m}$ single-mode fiber optic systems. A phase modulation effect wherein a single beam interferes with itself is used. PM to AM conversion occurs by mode-filtering in a single mode fiber. A factor of two increase in the optical modulation depth of the device is demonstrated using complementary drive of the parallel diodes comprising the device.

The authors wish to acknowledge fruitful discussions with B. Auld and the help of the Stanford University technical staff. This work is supported by JSEP/ONR under contract N00014-84-K-0327 and DARPA/ARO under DAAL03-88-K-0120.

REFERENCES

- [1] B. R. Hemenway, O. Solgaard, and D. M. Bloom, "All-silicon integrated optical modulator for 1.3 micron fiber-optic interconnects," *Appl. Phys. Lett.*, 24 July 1989.
- [2] D. Marcuse, "Loss analysis of single-mode fiber splices," *Bell Sys. Tech. J.*, Vol. 56, No. 5, June 1977, 713.
- [3] A. W. Snyder and J. D. Love, *Optical Waveguide Theory*, Chapman and Hall, New York, 1983, 504-506.
- [4] O. Solgaard, A. A. Godil, B. R. Hemenway, and D. M. Bloom, "Pigtailed fiber silicon light intensity modulator in a polarization-independent fiber link," unpublished.
- [5] B. R. Hemenway, H. K. Heinrich, J. H. Goll, and D. M. Bloom, "Optical detection of charge modulation in silicon integrated circuits using a multimode laser-diode probe," *Elec. Dev. Lett.*, 8, 8, Aug. 1987.
- [6] R. A. Soref, B. R. Bennett, "Electrooptical effects in silicon," *J. Quant. Elec.*, 23, 1, Jan. 1987.
- [7] D. Leenov, "The silicon pin diode as a microwave radar protector at megawatt levels," *IEEE Trans. Electron Devices*, 11, 53, (1964).
- [8] G. White, C. A. Burrus, "Efficient 100 Mb/s driver for electroluminescent diodes," *Int. J. Elec.*, 1973, 35, 6, pp. 751-754.
- [9] S. K. Ghandhi, *VLSI Fabrication Principles*, John Wiley & Sons, New York, 1983, p. 377.

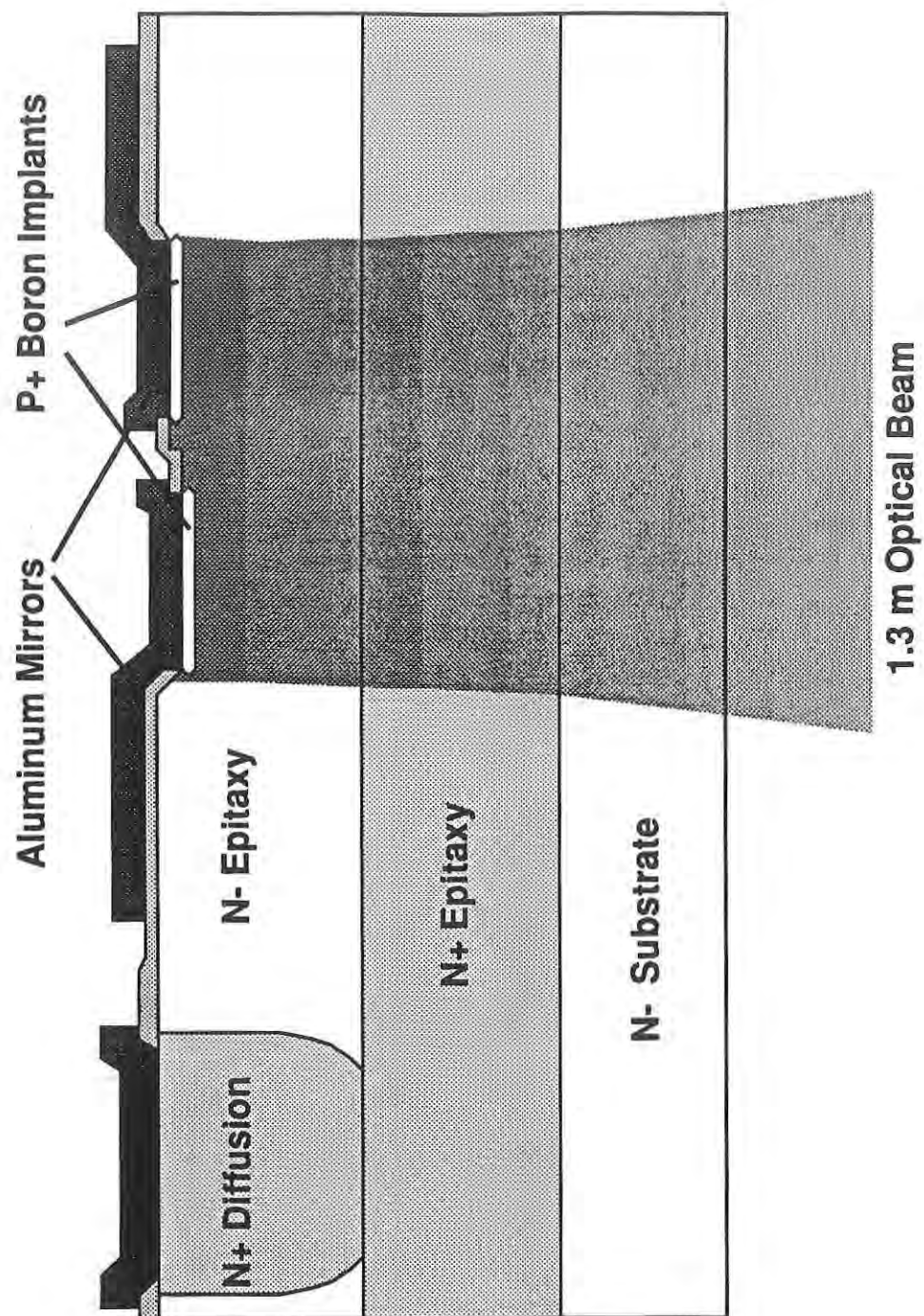


Fig. 1. Schematic cross section of push-pull modulator with light beam. Vertical diode on right has 454\AA phase bias built in.

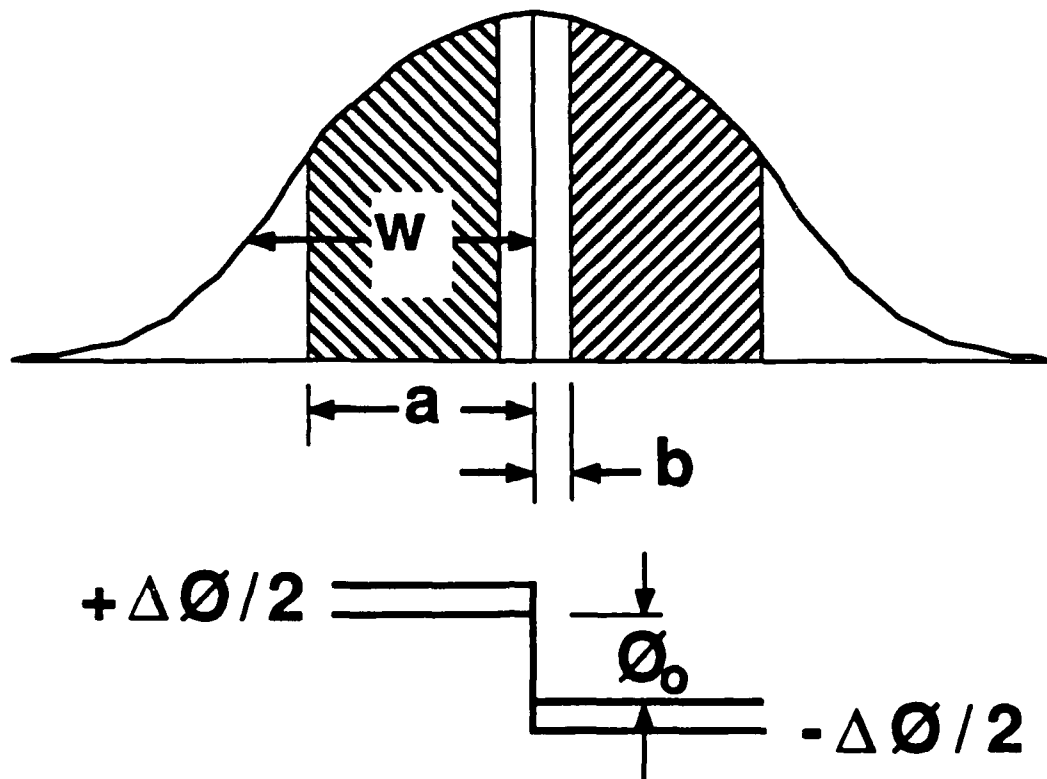


Fig. 2. Definition of geometric parameters used in gaussian beam modulation analysis. Upper figure shows electric field magnitude of input (clear) and reflected (shaded) gaussian beams. Dimension $a-b$ is diode contact mirror width. Lower figure shows phase of reflected beam. \varnothing_0 is the phase bias ($\pi/4$) and $\Delta\varnothing/2$ is the modulation per diode.

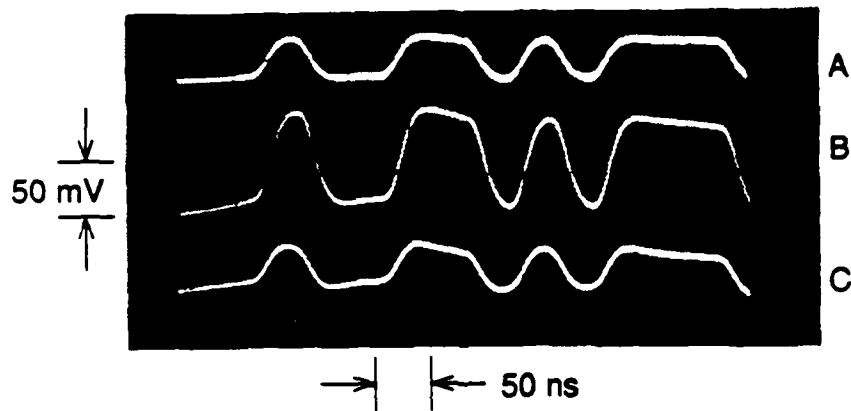


Fig. 3. Triple exposure of received oscilloscope traces showing push-pull operation. Trace "A" is received signal when data A is applied to the right hand diode of Fig. 1 only. Trace "C" is data $A\text{-bar}$ applied to the left hand diode only. Trace "B" shows result of A on right and $A\text{-bar}$ on left diodes simultaneously. No bias is applied.

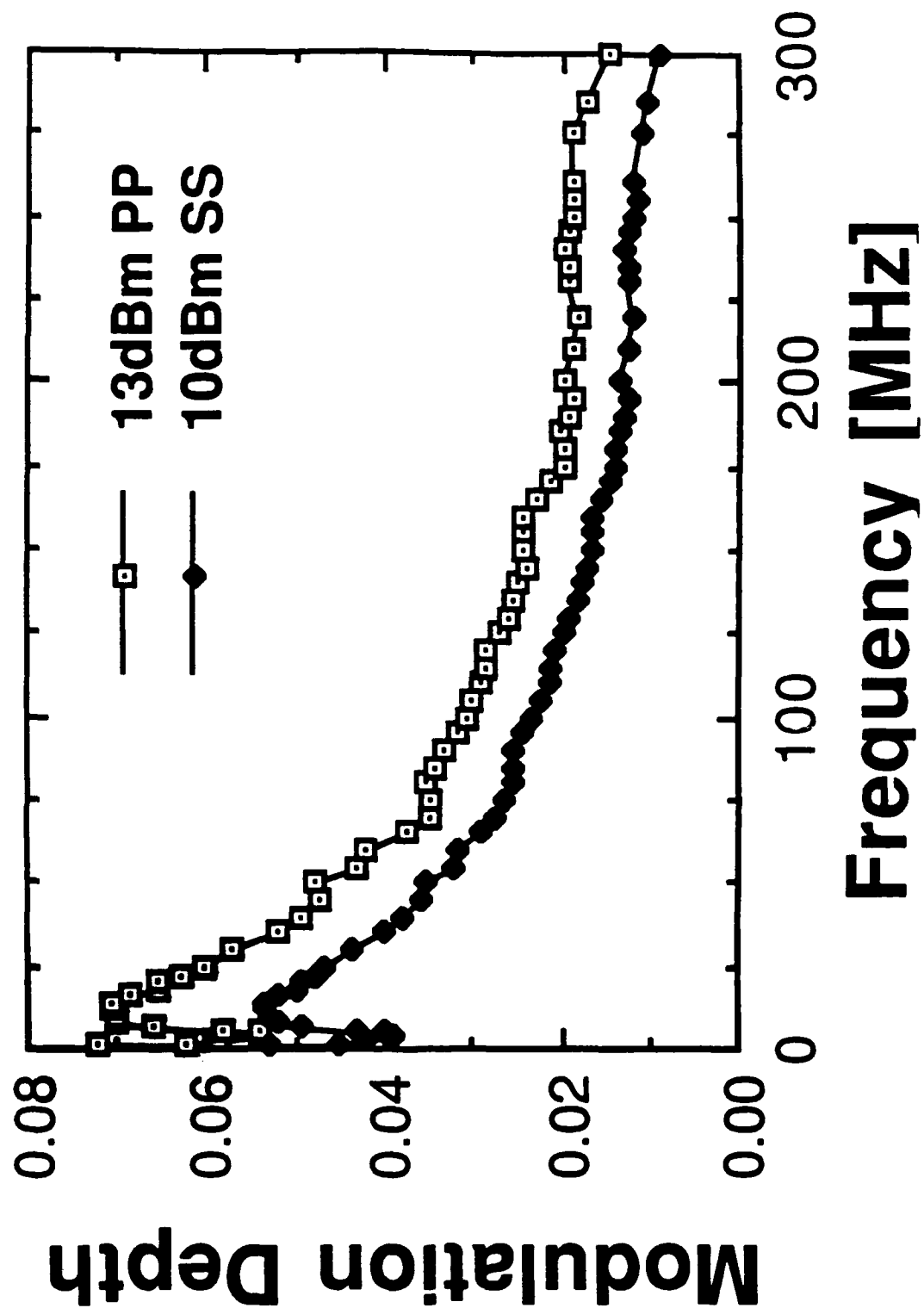


Fig. 4. Frequency response of push-pull (PP) modulator compared with response of the same device driven single-sided (SS). A bias of 7.8 mA is applied to the diode on the left in Fig. 1 and 11.3 mA is applied to the diode on the right.

Pigtailed single mode fiber optic light modulator in silicon.

O. SOLGAARD, STUDENT MEMBER, IEEE, A. A. GODIL, B. R. HEMENWAY, STUDENT MEMBER, IEEE, D. M. BLOOM, SENIOR MEMBER, IEEE.

The authors are with the

E. L. Ginzton Laboratory, Stanford University, Stanford, CA 94305.

Abstract.

We describe the performance of a light modulator at $1.3\text{ }\mu\text{m}$ wavelength based on the plasma effect in silicon. The modulator is directly coupled to a single mode fiber pigtail in a simple and robust package. The measured modulation index is 24 % with a 3 dB bandwidth of 60 MHz and the insertion loss is 5 dB. We see applications for this sensor in data acquisition from silicon sensors and other silicon IC's.

Introduction.

We have earlier reported a silicon light intensity modulator at $1.3\text{ }\mu\text{m}$ [1,2]. In this modulator one half of a zero order gaussian beam is phase delayed relative to the other half. This happens as the beam passes through a P-I-N diode where the charge density in the i-region is changed. The index of refraction and therefore the path length through the i-region is modulated by the plasma effect [3]. The charge is confined to one half of the beam by an isolating trench. The effect of this phase delay of one half of the beam relative to the other half, is to change the field distribution in the beam from a zero order gaussian to a sum of gaussians of order zero and higher. A static phase delay of $\pi/4$ is introduced in one half of the beam to maximize the response. When this modulated beam is coupled into a single mode fiber, only the fundamental gaussian mode will propagate. The phase modulation is thus converted to amplitude modulation by the mode selectivity of the single mode fiber.

The motivation for the work presented here is to demonstrate and characterize this silicon modulator in a fiber optical system with no bulk optical elements. To accommodate direct fiber pigtailling, the modulator has to match the mode size of the single mode fiber. The direct coupling and change in size have consequences for the modulation depth, frequency response and insertion loss of the modulator.

Experiment.

A schematic of the fiber pigtailed modulator are shown in figure 1. The modulator is fabricated using standard silicon IC technology. Light propagates from the single mode fiber through the silicon chip, is phase modulated and is then reflected back into the fiber off the metalization on the front side of the silicon chip. The silicon chip is mounted face down on the backside of the chip holder, and is wire bonded to through a hole in the holder. The package is filled with epoxy to give support during the thinning of the silicon chip. Thinning is necessary because the modulator does not have a waveguide, so the total propagation of the light before it is reflected back into the fiber must be less than the Rayleigh length, which in silicon is $260\text{ }\mu\text{m}$ for

a single mode fiber at 1.3 μm . If the unguided propagation length is significantly longer than this, the insertion loss will be prohibitively high. With the chip polished down to a thickness of 50 μm as in our pigtailed modulator, the insertion loss due to diffraction is about 0.36 dB [4].

The single mode fiber is glued in a glass capillary which is then polished to produce a clean fiber end. This assembly is then positioned over the modulator and glued with UV-epoxy while the modulation signal is monitored. The finished modulator package is shown in figure 2.

The total fiber optical system shown in figure 3. The source is a 1.3 μm distributed feedback laser with 3 mW output power. The 1.3 μm wavelength is chosen because it corresponds to the absorption minimum in silicon, but the modulator is inherently broadband. Since the total phase difference between the two halves of the beam is less than $\pi/2$, the demand on source coherence is not very strong. A light emitting diode or super luminescent diode would have a sufficiently narrow linewidth for this modulator.

The plasma effect is not dependent on the polarization state of the light and by using a regular 3 dB coupler, the overall system has a low polarization sensitivity. This is important in a fiber system since the polarization state tends to vary with fiber stress and temperature. The price we pay for the low polarization dependency, is the 6 dB power loss going through the 3 dB coupler twice. Note however that we could use two modulators, in which case only 3 dB of the power is wasted. The polarization independent coupler also leads to a large amount of power being reflected back towards the laser. Very good optical isolation of the laser diode is therefore required to avoid feedback induced noise in the semiconductor laser.

Results.

We obtained the strongest modulation driving the modulator with a DC current of 30 mA, corresponding to a current density of $6 \times 10^4 \text{ A/cm}^2$, and 22 mA rms of AC current, meaning the diode is just barely forward biased through out the cycle. Driving the modulator harder does not increase the signal because the stored charge is no longer confined to the active region of the modulator. The measured modulation depth is 24 %, and the frequency response has a single pole roll-off with the - 1.5 dB (3 dB electrical) point at 60 Mhz. Modulation depth is here defined as the peak-to-peak optical RF power over the maximum optical power during the cycle. The bandwidth of the modulator is primarily determined by the lifetime of the carriers.

The first generation pigtailed modulator does not have an AR coating at the fiber/silicon interface. Etalon effects can be neglected, due to high loss of multiple reflections. The primary reflected beam from the modulator suffers a 6 dB loss and is therefore comparable to the 15 % intensity reflection off the fiber/silicon interface. The interference of these two beams leads to a temperature dependence of the reflected light. The modulation depth as shown above, is measured with close to maximum reflected light from the modulator. This means that with an AR coating we expect the modulation depth to be twice the value we now measure.

The measured insertion loss of the modulator is 5 dB (when the two beams interfere constructively). The insertion loss for the light that is actually coupled into the modulator is then approximately 6 dB as stated above. The static phase delay is the cause of 3 dB of this loss, while only 0.36 dB is due to diffraction. The rest is caused by the trench that confines the charge to one half of the beam and by poor reflectivity of ohmic contact on front of silicon chip. The absorption in the silicon is negligible.

The noise level in the system is determined by the excessive laser noise due to feedback, so it would be advantageous to go to a LED or a solid state laser with low feedback sensitivity. We achieved the best signal to noise ratio with a non-planar ring neodymium YAG laser. With this source we configured the modulator system as a fiber optic link and demonstrated transmission of VHF TV signals with good quality.

Summary.

We have demonstrated a silicon light modulator at 1.3 μm wavelength in a fiber optic system. Because of the simple and robust package and the compatibility with silicon technology, this modulator provides an inexpensive interface between fiber optics and silicon IC's, with applications in data acquisition from silicon sensors.

Acknowledgement.

The authors would like to acknowledge assistance from J. Vrehl and P. Prather in the packaging of the modulator. This work was supported by DARPA/ARO under contract DAAL03-88-K-0120 and JSEP/ONR under contract N00014-84-K-0327.

References.

- [1] B.R. Hemenway, O. Solgaard, D.M. Bloom, "All-silicon integrated optical modulator for 1.3 μm fiber-optic interconnects", Appl. Phys. Lett. 55 (4), 24 July 1989.
- [2] B.R. Hemenway, O. Solgaard, A. A. Godil, D.M. Bloom, "A Polarization-independent Silicon Light Intensity Modulator for 1.32 μm Fiber Optics", to be published.
- [3] R.A. Soref, B.R. Bennet, "Electrooptical Effects in Silicon", IEEE J. of Quantum Electronics, QE-23, no. 1, p. 123 (1987).
- [4] D. Marcuse, "Loss analysis of single- mode fiber splices", Bell Sys. Tech. J., Vol. 56, No. 5, June 1977, 713.

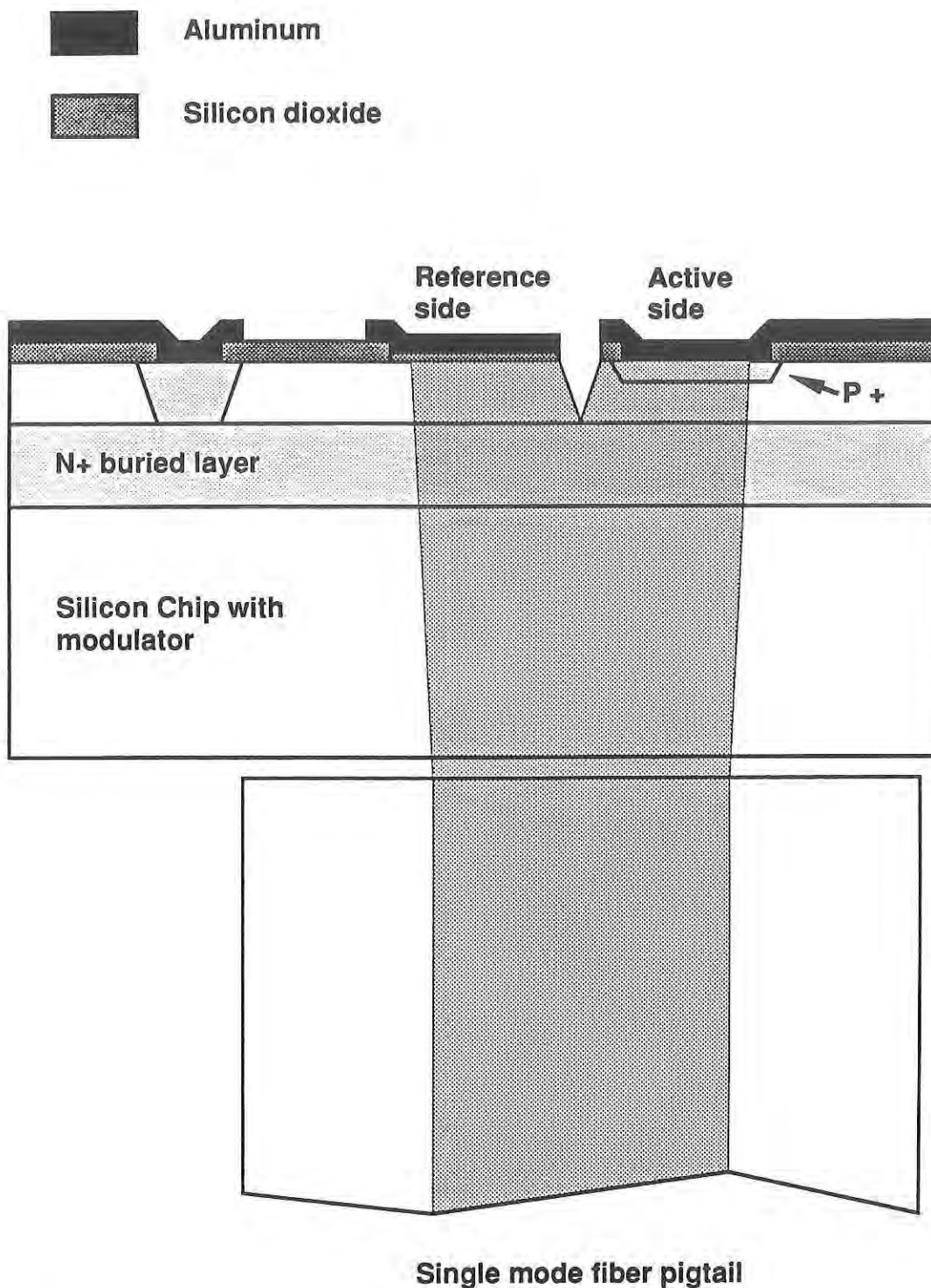


Figure 1. Schematic cross section showing the operational principle of the silicon modulator. The half of the beam that is reflected off the active side is phase modulated with respect to the other half. The result is that the optical field reflected back on the fiber is a sum of the fundamental gaussian mode and higher order modes. Only the fundamental propagates on the single mode fiber.

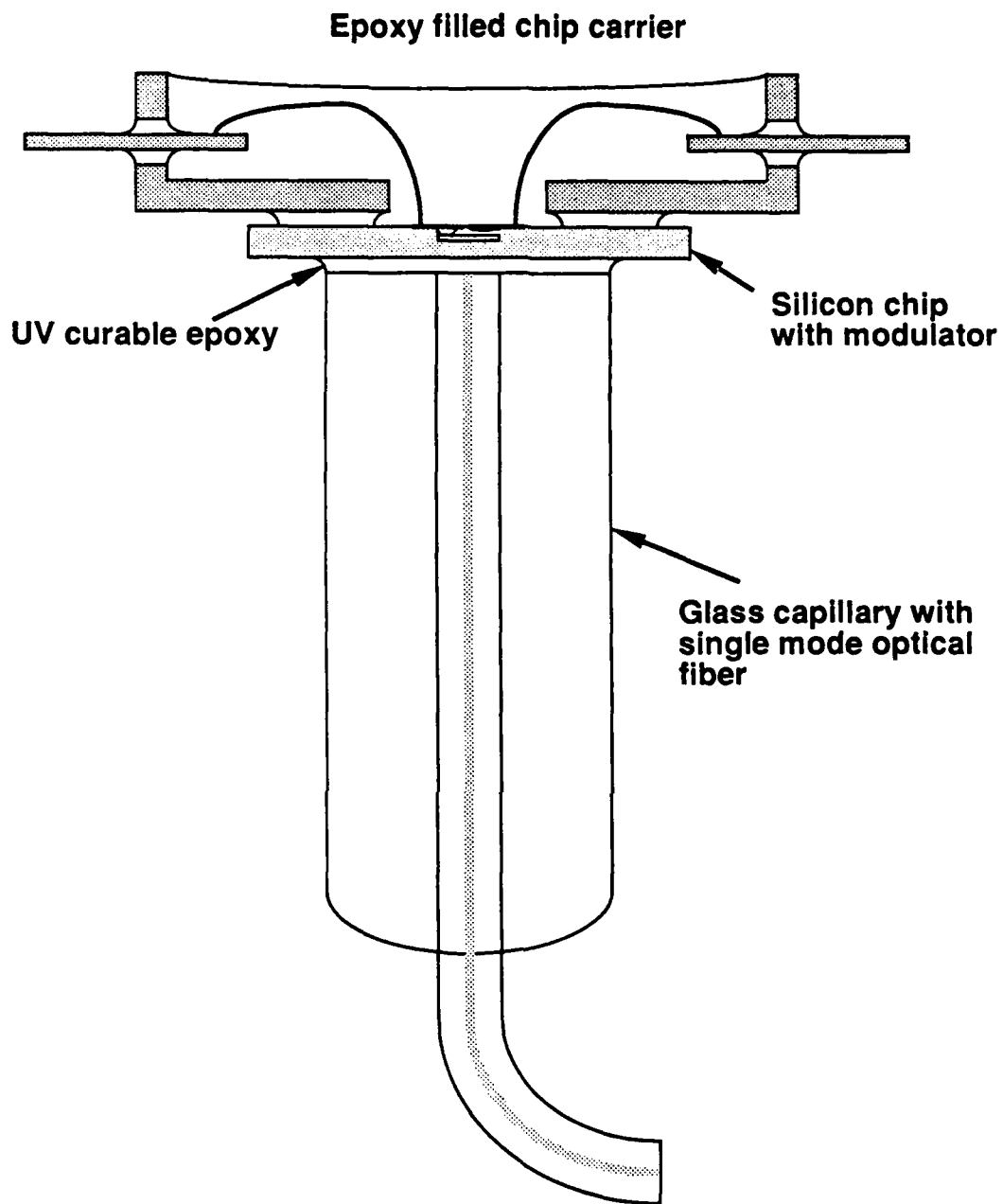


Figure 2. Schematic diagram showing the packaging of the modulator. The silicon chip is thinned down to $50\text{ }\mu\text{m}$, and the fiber pigtail in the capillary is glued directly to the back of the chip while the modulated signal is monitored.

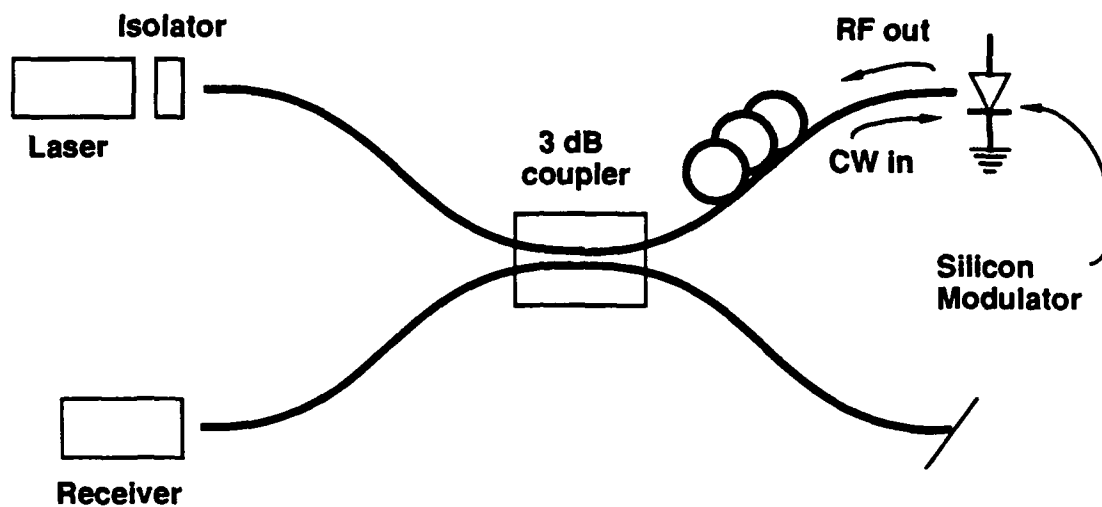


Figure 3. Fiber optic system employing the pigtailed silicon modulator. With a passive polarization independent power splitter as shown, the overall system is polarization independent.